J|A|C|S
ARTICLES
Published on Web 02/10/2004

Nature of Vibrational Coupling in Helical Peptides: An Isotopic Labeling Study

Rong Huang,[†] Jan Kubelka,[†] Wendy Barber-Armstrong,[‡] R. A. G. D. Silva,[‡] Sean M. Decatur,[‡] and Timothy A. Keiderling*[,†]

Contribution form the Department of Chemistry, University of Illinois at Chicago (m/c 111), 845 W. Taylor Street, Chicago, Illinois 60607, and Department of Chemistry, Mount Holyoke College, Carr Laboratory, S. Hadley, Massachusetts 01075

Received August 18, 2003; E-mail: tak@uic.edu

Abstract: Infrared (IR) and vibrational circular dichroism (VCD) spectra were measured for a series of isotopically (^{13}C on two or more amide C═O) labeled, 25 residue, α-helical peptides of the sequence Ac−(AAAAK)$_4$AAAAY−NH$_2$ that were also studied in the previous paper. Theoretical IR and VCD simulations were performed for correspondingly isotopically labeled Ac−A$_{24}$−NHCH$_3$ constrained to an α-helical conformation by use of property tensor transfer from density functional theory (DFT) calculations on Ac−A$_{10}$−NHCH$_3$. The simulations predicted and experiments confirmed that the vibrational coupling constants between *i*, *i* + 1 and *i*, *i* + 2 residues differ in sign, thus leading to a reversal of the ^{13}C VCD pattern and explaining the large shift in the ^{13}C amide I frequency as reported in the previous paper. The sign of the coupling constant remained consistent for larger label separation (with the exception of *i*, *i* + 4) and for more labels with uniform separation. Such effects confirm that the isotopically labeled group vibrations are essentially only coupled to each other and are effectively uncoupled from those of the unlabeled groups. This development confirms the utility of isotopic labels for site-specific structural studies with vibrational spectra. Observed spectral effects cannot be explained by considering only transition dipole coupling (TDC) between amide oscillators, particularly for smaller label separations, but the TDC and ab initio predicted couplings roughly converge at large separation.

Introduction

Understanding protein structure requires development of tools for detection of specific structural types. These are optimally tested and processed by analysis of measurements on peptides of uniform or well-defined structure. Vibrational spectroscopy has long been used to characterize secondary structures in peptides and proteins.[1] Infrared (IR) and Raman analyses take advantage of more highly resolved spectral components than possible with electronic spectroscopies and of the multiple transitions characteristic of the vibrational region by assigning the components to specific structural types.[2] In the past decade, vibrational circular dichrosim (VCD) and its counterpart, Raman optical activity (ROA), were also applied to secondary structure analysis, thereby transferring the wider band shape variation characteristic of a differential spectroscopy like (electronic) circular dichroism (CD)[3] to resolved vibrational transitions now possessing a sign dependence that originates in the conformation.[4,5]

The influence of secondary structure on the frequencies of characteristic amide-based vibrational excitations has been the prime source of their structural utility in IR and Raman measurements. In the IR, most effort focused on the conformationally dependent frequency of the amide I mode (primarily amide C═O stretch), due to its high intensity and its freedom from spectral overlap with other modes. While much has been assumed as to the origin of these frequency shifts, recent detailed, quantum mechanically based, force field (FF) calculations on small peptides have shown that coupling between the amides is the dominant stereochemical interaction that must be properly modeled.[6−11] Hydrogen bonding effects and solvation perturbations are significant, such as seen for α-helices in water,[12] but the coupling of local modes through the secondary structure is a fundamental characteristic of the conformation

[†] Department of Chemistry, University of Illinois at Chicago.
[‡] Department of Chemistry, Mount Holyoke College.

(1) Keiderling, T. A.; Silva, R. A. G. D. In *Synthesis of Peptides and Peptidomimetics*; Goodman, M., Felix, A., Moroder, L., Toniolo, C., Eds.; Georg Thieme Verlag: Stuttgart, 2002; Vol. E22b, pp 715−738.
(2) Mantsch, H. H.; Chapman, D. *Infrared Spectroscopy of Biomolecules*; Wiley-Liss: Chichester, UK, 1996.
(3) Venyaminov, S. Y.; Yang, J. T. In *Circular Dichroism and the Conformational Analysis of Biomolecules*; Fasman, G. D., Ed.; Plenum Press: New York, 1996; pp 69−107.
(4) Keiderling, T. A. In *Circular Dichroism: Principles and Applications*, 2nd ed.; Berova, N., Nakanishi, K., Woody, R. A., Eds.; Wiley-VCH: New York, 2000; pp 621−666.
(5) Barron, L. D.; Hecht, L. In *Circular Dichroism: Principles and Applications*, 2nd ed.; Berova, N., Nakanishi, K., Woody, R. W., Eds.; Wiley-VCH: New York, 2000; pp 667−701.
(6) Kubelka, J.; Bour, P.; Silva, R. A. G. D.; Decatur, S. M.; Keiderling, T. A. In *Chirality: Physical Chemistry*; ACS Symposium Series 810; Hicks, J. M., Ed.: Washington, DC, 2002; pp 50−64.
(7) Bour, P.; Kubelka, J.; Keiderling, T. A. *Biopolymers* **2000**, *53*, 380−395.
(8) Bour, P.; Keiderling, T. A. *J. Am. Chem. Soc.* **1993**, *115*, 9602−9607.
(9) Kubelka, J.; Keiderling, T. A. *J. Am. Chem. Soc.* **2001**, *123*, 12 048−12 058.
(10) Jalkanen, K. J. *J. Phys.: Condens. Matter* **2003**, *15*, S1823−1851.
(11) Schweitzer-Stenner, R.; Eker, F.; Huang, Q.; Griebenow, K. *J. Am. Chem. Soc.* **2001**, *123*, 9628−9633.
(12) Martinez, G.; Millhauser, G. L. *J. Struct. Biol.* **1995**, *114*, 23−27.

10.1021/ja037998t CCC: $27.50

and is vital to vibrational spectroscopic analysis. Thus, to optimally utilize IR spectra for structural studies, it is critical to develop a basic understanding of this coupling.

Interresidue coupling is most dramatically seen in the large ($\geq$60 cm^{-1}) splitting of antiparallel β-sheet amide I modes.[9,13,14] However, as has been pointed out by several researchers, finite helical peptides also have intensity components dispersed over a wide range of frequencies.[6,7,13,15] In principle, this can interfere with interpretation of spectra both qualitatively, by confusing assignments for structural components of much smaller contribution, and quantitatively, by spreading intensity into regions assigned to other components.[6,16] Proper modeling of the dispersion of spectral response for any given conformational type will depend on solid understanding of coupling mechanisms.

A problem in any approach based on analyzing vibrational spectra to yield detailed coupling information is the difficulty in resolving contributions from individual residues. Several recent studies have addressed such coupling interactions for tripeptides which have only two interacting amide groups that are distinct by being on opposite termini of the peptide.[11,17−20] While such peptides have been assigned to a dominant 3_1-helical (poly Proline II-like) structure, they are certainly fluctional and have less well-defined conformations than residues forming the dominant structure elements of proteins, such as α-helices and β-sheets. However, these structures in turn require larger peptides to develop stable conformers.[21] In addition, contributions of different structural components in proteins are likely to interfere due to the dispersed intensity as the segments in a globular fold necessarily get shorter and more deformed.

We have been able to study vibrational spectra of conformationally stable, specific residue peptide sequences in α-helices (and other structures) by use of isotopic labeling.[9,22−26] Substitution of ^{13}C onto a single amide C═O leads to a shift for the amide I mode in an α-helix of $\sim$40 cm^{-1} lower in wavenumber, resulting in spectral resolution of the ^{13}C labeled modes from the ^{12}C modes.[6,22−29] Such shifts are different for various structures and for multiple substitutions due to local and extended coupling. A single residue shift should reflect the position of the amide I in the absence of interresidue coupling, assuming that the ^{13}C residue is an isolated probe of the structure. Isotopic substitution provides an opportunity to experimentally test the conformation of a specific, local segment of the peptide and to critically assess theoretical simulations of peptide vibrational spectra. In addition, since the IR contributions of as few as two residues in long helical or sheetlike peptides (>20 residues) can be easily detected,[6,25−28] one can use the spectra of such isotopic labels to obtain direct information about residue coupling in well-defined structures. Such tests of theoretical models of vibrational interaction avoid the structural ambiguities inherent in the study of very small peptides.[11,17−19] Initial IR studies of ^{13}C labeled helical peptides reported the expected shift from the ^{12}C amide I band,[22,23] but sheetlike models showed more variations.[27,28] This variance implied that frequency could only be associated with a specific conformational type by independently knowing the overall structure and thus that of residues in the labeled part of that structure. With VCD, that ^{13}C-shifted band is given a conformationally sensitive shape which enables definitive conformational assignment for a specific segment of the peptide.[6,24] Previous studies were based on an implicit assumption that the ^{13}C labeled vibrations are effectively decoupled from the rest of the peptide. In this paper, we provide experimental and theoretical evidence that such an assumption is valid for the most part, and thus show that ^{13}C labeling provides an ideal local probe of stereochemistry when interrogated with vibrational spectroscopy.

Our previous studies of isotope labeled helical peptides focused on the positional sensitivity of IR and VCD spectra for four ^{13}C labeled residues placed at positions in the sequence varying from the N- to C-terminus[24] and on their theoretical simulation.[7,25] By contrast, in the present study, all labeled residues are in a helical conformation since they are restricted to the center segments of a 25 residue peptide, Ac−(AAAAK)$_4$AAAAY−NH$_2$, (A = Ala, K = Lys, Y = Tyr), which in aqueous solution at low temperatures forms a quite stable helix. Experimental IR and VCD spectra for this peptide modified with sequential (nearest neighbor), alternate (next nearest neighbor) and more highly spaced arrangements of two to four labeled residues are reported. These spectra are simulated using our property tensor transfer methods,[30] in this case based on ab initio computation of spectral parameters for an α-helical model peptide, Ac−A$_{10}$−NHCH$_3$, which, to our knowledge, is longer than has been used in any previous DFT-based simulation of peptide vibrational spectra.[6,21,24] The agreement between experiment and theory is excellent and leads to development of an interpretation for the coupling mechanism in these residues.

Materials and Methods

Materials. A series of alanine-rich peptides (25 residues) were synthesized and purified at Mount Holyoke College by standard solid-phase methods as described previously.[22,31] The general form of the blocked peptides is Ac−(AAAAK)$_4$−AAAAY−NH$_2$. Ala residues with ^{13}C isotopic labels on the C═O were inserted into the sequence at various positions as shown in Table 1. All the peptides were deuterium exchanged and had TFA removed by lyophilization from a deuterated phosphoric acid solution (0.1%). Peptide samples were then dissolved in D_2O to a concentration of $\sim$25 mg/mL (pH $\approx$ 2) for spectral measurements. D_2O was purchased from Cambridge Isotope Laboratories, Cambridge, MA.

(13) Krimm, S.; Bandekar, J. *Adv. Protein Chem.* **1986**, *38*, 181−364.
(14) Miyazawa, T. *J. Chem. Phys.* **1960**, *32*, 1647−1652.
(15) Torii, H.; Tasumi, M. *J. Chem. Phys.* **1992**, *96*, 3379−3387.
(16) Pancoska, P.; Wang, L.; Keiderling, T. A. *Protein Sci.* **1993**, *2*, 411−419.
(17) Eker, F.; Cao, X.; Nafie, L.; Schweitzer-Stenner, R. *J. Am. Chem. Soc.* **2002**, *124*, 14 330−14 341.
(18) Woutersen, S.; Hamm, P. *J. Phys. Chem. B* **2000**, *104*, 11 316−11 320.
(19) Woutersen, S.; Hamm, P. *J. Chem. Phys.* **2001**, *114*, 2727−2737.
(20) Woutersen, S.; Hamm, P. *J. Phys.: Condens. Matter* **2002**, *14*, R1035−1062.
(21) Bour, P.; Kubelka, J.; Keiderling, T. A. *Biopolymers* **2002**, *65*, 45−59.
(22) Decatur, S. M.; Antonic, J. *J. Am. Chem. Soc.* **1999**, *121*, 11 914−11 915.
(23) Decatur, S. M. *Biopolymers* **2000**, *54*, 180−185.
(24) Silva, R. A. G. D.; Kubelka, J.; Decatur, S. M.; Bour, P.; Keiderling, T. A. *Proc. Natl. Acad. Sci. U.S.A.* **2000**, *97*, 8318−8323.
(25) Setnicka, V.; Hammer, R. P.; Keiderling, T. A. To be submitted.
(26) Kubelka, J.; Keiderling, T. A. *J. Am. Chem. Soc.* **2001**, *123*, 6142−6150.
(27) Halverson, K.; Sucholeiki, I.; Ashburn, T. T.; Lansbury, R. T. *J. Am. Chem. Soc.* **1991**, *113*, 6701−6703.
(28) Brauner, J. W.; Dugan, C.; Mendelsohn, R. *J. Am. Chem. Soc.* **2000**, *122*, 677−683.
(29) Moran, A. M.; Park, S.-M.; Dreyer, J.; Mukamel, S. *J. Chem. Phys.* **2003**, *118*, 3651−3659.
(30) Bour, P.; Sopkova, J.; Bednarova, L.; Malon, P.; Keiderling, T. A. *J. Comput. Chem.* **1997**, *18*, 646−659.
(31) Barber-Armstrong, W.; Donaldson, T.; Wijesooriya, H.; Decatur, S. M.; Silva, R. A. G. D. *J. Am. Chem. Soc.* **2004**, *126*, 2339−2345.

Table 1. Peptide Sequences

notation	peptide sequence[a]
unlabeled	Ac−AAAAKAAAAKAAAAKAAAAKAAAAY−NH_2
1L	Ac−AAAAKAAAAK***A***AAAKAAAAKAAAAY−NH_2
2LT	Ac−AAAAKAAAAK***AA***AAKAAAAKAAAAY−NH_2
2L1S	Ac−AAAAKAAAAK***A***AA***A***AKAAAAKAAAAY−NH_2
2L2S	Ac−AAAAKAAAAK***A***AA***A***KAAAAKAAAAY−NH_2
2L3S	Ac−AAAAKAAA***A***KAA***A***AKAAAAKAAAAY−NH_2
2L4S	Ac−AAAAKAA***A***AKAA***A***AKAAAAKAAAAY−NH_2
2L5S	Ac−AAAAKAA***A***AKAAA***A***KAAAAKAAAAY−NH_2
2L6S	Ac−AAAAKAAA***A***KAAAAK***A***AAAKAAAAY−NH_2
2L7S	Ac−AAAAKAA***A***AKAAAAK***A***AAAKAAAAY−NH_2
3LT	Ac−AAAAKAAAAK***AAA***AKAAAAKAAAAY−NH_2
3L1S	Ac−AAAAKAAA***A***K***A***AA***A***AKAAAAKAAAAY−NH_2
4LT	Ac−AAAAKAAAAK***AAAA***KAAAAKAAAAY−NH_2
4L1S	Ac−AAAAKA***A***A***A***K***A***AA***A***AKAAAAKAAAAY−NH_2

[a] Italic residues are ^{13}C labeled on the amide C═O.

Spectral Measurements. Mid-IR absorption spectra were measured using a Digilab FTS-60A FTIR spectrometer with a DTGS detector at 4 cm^{-1} resolution as an average of 1024 scans. VCD spectra were measured on the UIC dispersive VCD instrument which has been described in detail.[32,33] The solution samples were placed in a homemade demountable cell consisting of a 50 μm Teflon spacer sandwiched between CaF_2 windows and sealed in a brass ring which was held in a variable temperature mount.[34] The VCD spectra were recorded with 10 cm^{-1} spectral resolution and the spectra used here were an average of eight scan accumulations. Baseline spectra for just D_2O contained in the same cell were measured in an identical procedure as were the samples for both VCD and IR. The baseline spectra were subtracted from the averaged sample spectra at each temperature for presentation in the Figures.

Computations. To understand the nature of these IR and VCD spectra of isotopically substituted peptides, we have simulated them theoretically using our established methods for spectral property tensor transfer.[6,30] In this set of calculations, an ab initio quantum mechanical force field (FF) and atomic polar and axial tensors (APT and AAT) were computed with density functional theory (DFT) methods at the BPW91/6-31G* level for Ac−A_{10}−$NHCH_3$. An idealized α-helical secondary structure ($\phi = -57°$, $\psi = -47°$, $\omega = 180°$) was the only constraint and all other geometrical parameters were fully energy optimized. This 11-amide model peptide is one full α-helical turn longer than our previously used 7-amide model,[6,24,35] which allows simulation of some minor length effects for the resultant spectra, particularly for VCD. The FF, APT, and AAT parameters obtained for this model were then transferred onto Ac−A_{24}−$NHCH_3$, a full-length peptide appropriate for modeling the samples studied experimentally. Spectra were simulated by diagonalizing the resultant full-peptide FF matrix with appropriate isotopic substitutions. The difference in vibrational frequencies of isolated oscillators was used to indicate their coupling (the labeling assumption). The APT and AAT values were used to simulate IR and VCD intensities by assigning Lorentzian band profiles with 20 cm^{-1} full-width at half-maximum (fwhm) to each transition and summing to yield realistic band shapes.

In this investigation, computations actually suggested the experimental design, thus simulation results represent true "predictions" by theory and can be legitimately presented first followed by experiment. Since the VCD experiments in particular were quite challenging, comparison with the simulation can enhance identification and assignment of transitions. As with all computational models of spectra, these do have limitations. Because the DFT calculations are done for isolated (vacuum) molecules, the frequencies (especially for the C═O stretch, due to neglect of solvent[36]) are high compared to experimental values obtained in aqueous solution. Previous work has shown this to result in primarily a shift of the band, as there is little band shape change for these helical peptides due to water solvation effects.[6,35−38] Due to solvent interference problems with H_2O, all these spectra were measured in D_2O and the peptides were preexchanged to the N−D form. This leads to a shape change in the amide I′ VCD from a positive couplet to a three-peaked (−, +, −) band shape.[4,39,40] Our previous simulations based on calculations for helical peptides only in a vacuum have not succeeded in reproducing this third amide I′ feature (negative band to low frequency) under N-deuteration conditions alone. However, as reported separately,[37,38] we can simulate such band shape results by hydrating the helix and calculating the VCD spectra with explicit waters, although, experimentally, aqueous solution is not required to observe the effect. Thus, knowing that the main inadequacy of the FF is reproduction of absolute frequency, we here focus on the relative ^{13}C induced shifts of the VCD band from the main ^{12}C amide I feature and on the relative VCD band shapes between the two isotopically shifted bands. There is little or no isotope effect predicted for the amide II (N−H deformation + C−N stretch), so no data regarding that feature is presented. In addition IR and VCD of the amide III are too weak and too complicated by mixing with other modes to be considered for this study of coupling.

Transition Dipole Coupling (TDC) Calculations. To understand better the physical origin of the coupling computed between ^{13}C labeled residues with our ab initio FF, we carried out a series of TDC-based calculations for comparison. These used geometry parameters appropriate for an idealized α-helix, such as used for our ab initio calculations above, with the transition dipole moments located on the amide carbonyls and oriented along the bond axis. In the TDC formalism, the energy splitting is $2V_{ab}$ (the coupling matrix element, as determined in eq 1 of the previous paper[31]).

In this model, the rotational strengths, $R^{\pm}$, for the symmetric and asymmetric coupled modes are as follows

$$R^{\pm} = \mp(\pi\nu/2c)T_{ab}\cdot(\mu_a \times \mu_b) \qquad (1)$$

where μ_a, μ_b are the vector dipole moments and T_{ab} is the vector from dipole a to b, ν is the unperturbed transition frequency (s^{-1}) and c is the speed of light.[41,42]

(32) Keiderling, T. A. In *Practical Fourier Transform Infrared Spectroscopy*; Krishnan, K., Ferraro, J. R., Eds.; Academic Press: San Diego, 1990; pp 203−284.
(33) Keiderling, T. A.; Hilario, J.; Kubelka, J. In *Vibrational Spectroscopy of Polymers and Biological Systems*; Braiman, M., Gregoriou, V., Eds.; Marcel Dekker: Amsterdam, New York (in press).
(34) Wang, L. Ph.D. Thesis, Department of Chemistry, University of Illinois at Chicago: Chicago, 1993.
(35) Kubelka, J.; Silva, R. A. G. D.; Keiderling, T. A. *J. Am. Chem. Soc.* **2002**, *124*, 5325−5332.
(36) Kubelka, J.; Keiderling, T. A. *J. Phys. Chem. A* **2001**, *105*, 10 922−10 928.
(37) Bour, P.; Keiderling, T. A. *J. Chem. Phys.* **2003**, in press.
(38) Kubelka, J.; Keiderling, T. A. **2003**, to be submitted.
(39) Sen, A. C.; Keiderling, T. A. *Biopolymers* **1984**, *23*, 1533−1545.
(40) Yasui, S. C.; Keiderling, T. A. *Biopolymers* **1986**, *25*, 5−15.
(41) Holzwarth, G.; Chabay, I. *J. Chem. Phys.* **1972**, *57*, 1632−1635.
(42) Tinoco, I. *Radiat. Res.* **1963**, *20*, 133−139.

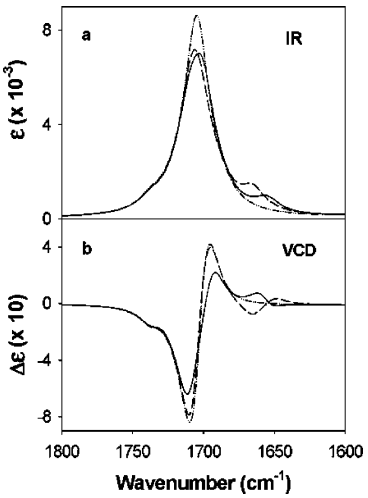

Figure 1. Simulated amide I′ FTIR (a) and VCD (b) spectra for the unlabeled (dash−dotted line −••−••−), compared to the sequential, 2LT (dash line − − −) and alternate, 2L1S (solid line ——) doubly labeled Ac−A_{24}−$NHCH_3$ in the α-helical conformation. The difference in the 2LT and 2L1S ^{13}C amide I′ positions is predicted to be 10 cm^{-1}.

We assume that the two amide oscillators are degenerate and use the theoretically obtained value of 0.054 D^2 for the dipolar strength and 1656 cm^{-1} (from our simulation) for the frequency of the unperturbed single ^{13}C amide I. The splitting and shift analysis in the previous paper[31] employed empirical values for the structure (derived from averages for protein helices) and dipole strength which explains the deviations between the two TDC computations.

Results

In Figure 1 are compared the simulated amide I IR and VCD spectra for Ac−A_{24}−$NHCH_3$ and its isotopomers where two ^{13}C-labels are substituted both sequentially and alternately on the C═O group of the center residues. The ^{13}C substitution causes the ^{12}C IR band to lose intensity and shift in frequency (Figure 1a), with the sequential isotopomer ^{12}C shifting up ∼2 cm^{-1} and the alternate one being lower by ∼4 cm^{-1}. However, the main effect of isotopic placement is evident in the ^{13}C features, which differ by ∼10 cm^{-1} due to the intensity distribution between the two vibrational modes. The higher frequency component is more intense in the sequentially labeled peptide, but less intense in the alternately labeled one, thus resulting in its lower frequency ^{13}C absorbance maximum. The lower ^{13}C frequency calculated for the alternate isotopomer is only ∼2 cm^{-1} lower than that predicted for a singly labeled peptide and is about the same as for peptides with labels separated by two residues. However, for a three residue separation the ^{13}C band shifts higher than that for the single labeled peptide (as compiled in Table 2 and illustrated in Figure 2). These patterns are qualitatively the same as seen experimentally in the preceding paper.[31]

The difference between these IR spectra for different separations results from the stronger coupling of local modes on neighboring ^{13}C-labeled residues as opposed to that between labeled C═O's with intervening ^{12}C residues. The dramatic shift in the observed IR for 2LT to 2L1S comes about because the sign of the coupling, V_{ab}, changes, which results in the more intense in-phase mode being higher in frequency of the pair for sequential substitution and lower for alternate substitution. Clearly, the degree of such coupling in a simulated spectrum is a function of the FF used. Experiment provides the clearest test of the predictability of our FF, and the relevant results are shown in Figure 3 for Ac−$(AAAAK)_4AAAAY$−NH_2 and its 2LT and 2L1S isotopomers at 2 °C. The predicted difference of 10 cm^{-1} for the sequential and alternate labels is seen experimentally (Figure 3a), with the sequential substitution being higher in frequency (closer to the ^{12}C band). The measured absolute molar intensities are not very reliable, due to difficulties in weighing small samples, correcting for impurities and maintaining a constant path length, therefore the spectra were normalized to a constant amide I′ area. Normalized IR indicate some intensity loss in the ^{12}C band when two residues are labeled and show the predicted result that the ^{13}C band for sequential substitution is higher in frequency than for alternate substitution, as shown in the previous paper.[31]

In the VCD spectra, the predicted and observed difference between the sequential and alternate isotopomers is more dramatic. As shown in Figure 1b, the simulated VCD spectra for the ^{13}C band of the sequentially labeled peptide has the same sign pattern as for the ^{12}C (both being positive couplets characteristic for right-handed helices), but the opposite ^{13}C sign pattern (at nearly overlapping frequencies) is seen for the alternate labeled peptide. The spectral overlap for these two isotopomers and their relative ^{13}C sign change are again direct consequences of the sign reversal for the coupling term and the resultant inversion of the in- and out-of-phase mode ordering between the two substitution patterns. In both cases the in-phase component has negative VCD and the out-of-phase positive VCD. The alternate substitution is also predicted to have a much larger impact on the ^{12}C band, reducing its VCD intensity, which we discuss in more detail later. Such small VCD signals as predicted, arising from just two labels out of 26 amides in the molecule, are difficult to measure, but the experimental results in Figure 3b fully support the simulations when one accounts for the extra negative feature to low frequency of the ^{12}C band, which is not present in the simulation.[6] Here, it is important to point out that the ^{13}C VCD is virtually overlapped for the two isotopomers, giving rough mirror-image patterns, at ∼1587 and 1602 cm^{-1}, just as in the simulation. It must be recognized that this apparent splitting in oppositely signed VCD peaks is not a measure of the splitting but rather is a function of the line width for overlapped transitions. The important sign change between these two substitution patterns is diagnostic since it occurs in both experiment and simulation, is carried through for multiple labeled peptides, and must reflect the fundamental characteristic of mode coupling, as we discuss later.

One variable that we can use to empirically evaluate coupling is the distance between labeled residues, both through the peptide chain (mechanical) and through space (dipolar). As the distance between isotopic labels changes, the strength of the transition dipole coupling (TDC) changes in a predictable manner. By contrast, mechanical coupling will fall off very fast as a function of adding interspersed residues, but for the sequential labeling case, it is presumably a primary source of amide I coupling. To illustrate this, in Figure 2 are plotted the ^{13}C band and underlying mode positions for one and two labeled oligomers. The mode distribution demonstrates that with increased label separation, the predicted IR peak position of the ^{13}C band does vary initially, but approaches a constant

Table 2. Comparison of Quantum Mechanical (QM) Simulations and Transition Dipole Coupling (TDC) Model Calculations

peptide notation	^{13}C═Os angle (°)	^{13}C═Os separation T_{ab} (Å)	^{12}C simulated peak shift[a,b] (cm^{-1})	^{13}C simulated peak shift[a,c] (cm^{-1})	QM frequencies for ^{13}Cs (cm^{-1})	QM pred. D (Debye^2)	QM pred. effective V_{ab} (cm^{-1})	TDC pred. V_{ab} (cm^{-1})	QM pred. R^{+} [e]	TDC pred. R^{+} [e]
unlabeled			0[b]							
1L			−1	0[c]	1656.6	0.053				
2LT	25	3.3	2.5	8.9	1665.5 (s)[d]	0.150	7.6	4.6	−474	−86
					1650.3 (a)[d]	0.007				
2L1S	34	4.9	−3.8	−1.7	1659.3 (a)	0.020	−2.4	−0.7	−468	−135
					1654.4 (s)	0.082				
2L2S	18	5.2	−0.4	−1.7	1658.9 (a)	0.006	−2.0	−3.2	−5	9
					1654.8 (s)	0.097				
2L3S	12	6.6	0.6	0.8	1657.4 (s)	0.111	0.6	−1.4	−64	−57
					1656.3 (a)	0.003				
2L4S	35	8.7	1.8	0	1657.6 (a)	0.020	−0.6	−0.5	−571	−206
					1656.4 (s)	0.088				
2L5S	34	10.2	−2.1	0.2	1657.4 (a)	0.019	−0.4	−0.4	−217	−24
					1656.6 (s)	0.090				
2L6S	9	11.2	−0.5	0.4	1657.2 (a)	0.015	−0.1	−0.3	175	63
					1656.9 (s)	0.095				
2L7S	22	13.2	−0.6	0.6	1657.7 (a)	0.035	−0.4	−0.2	−134	−218
					1656.9 (s)	0.073				

[a] Frequencies are determined by 2nd derivative of the simulated IR spectra. [b] ^{12}C frequency (in wavenumber) is referenced to unlabeled peptide for easier comparison (the computed ^{12}C frequency of the unlabeled peptide is 1704.5 cm^{-1}). [c] ^{13}C frequency (in wavenumber) is referenced to 1L for easier comparison (the computed ^{13}C frequency of 1L is 1656.3 cm^{-1}). [d] "s" means in-phase mode and "a" means out-of-phase mode. [e] R^{+} in units of 10^{-8} Debye^2 for the symmetric component.

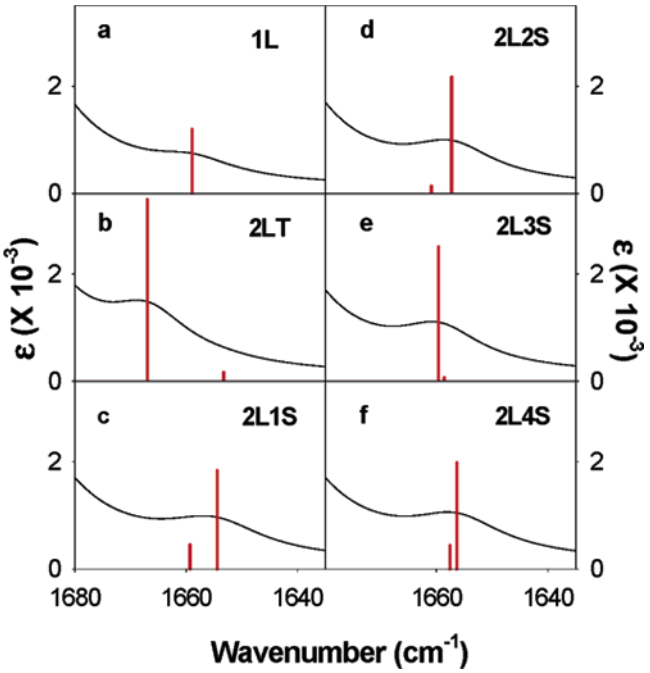

Figure 2. Simulated ^{13}C amide I′ FTIR spectra and normal mode contributions for (a) 1L; (b) 2LT; (c) 2L1S; (d) 2L2S; (e) 2L3S; and (f) 2L4S. The coupling of the two ^{13}C═Os is interpreted to be half the splitting of the ^{13}C modes.

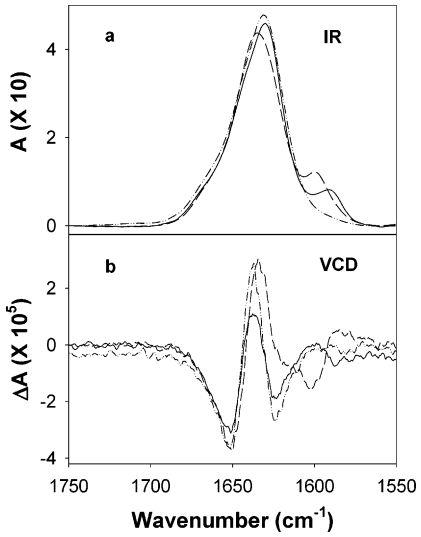

Figure 3. Amide I′ FTIR (a) and VCD (b) spectra for the unlabeled (dash−dotted line −••−••−), 2LT (dash line − − −) and 2L1S (solid line ——) peptides at 2 °C. (Spectra are normalized to have the same integral amide I′ peak area.) Experimental spectra confirmed the predicted 10 cm^{-1} difference in the ^{13}C amide I′ bands for the sequential and the alternate isotopomers and the distinct sign of the VCD patterns for these two isotopomers. The VCD spectrum of the unlabeled peptide is offset by −3 × 10^{-6} for better baseline comparison.

frequency. The splitting goes to zero for large label separations, which is consistent with a loss of mechanical and dipolar coupling between labeled residues. The through-space distance between ^{13}C═O groups is about the same for the $i \rightarrow i + 2$ and $i \rightarrow i + 3$ labeling in 2L1S and 2L2S, respectively, and the computed splitting for both is 4−5 cm^{-1}. Both distances are substantially more than the sequential, $i \rightarrow i + 1$, separation which has a predicted splitting of ∼15 cm^{-1}. However, the $i \rightarrow i + 4$ through-space distance is again substantially more, despite the helical relationship and the H-bond connection between C═O (i) and N−H ($i + 4$), which results in a much smaller (∼1−2 cm^{-1}) computed splitting, suggesting dominance by dipolar coupling at these separations. The symmetric and asymmetric modes for 2L3S are reversed as compared to our predictions for all the other 2LnS, $n = 1-7$, doubly labeled peptides. The distances (T_{ab}) along with the angular relationships of the coupled transition dipoles, the peak frequency variations (both ^{12}C and ^{13}C), and other related information (energy splitting, dipole strength, rotational strength) are summarized in Table 2. It is clear that for 2L3S the experimental ^{13}C IR peak shifts back to higher wavenumbers (Table 3), which is predicted in the quantum mechanical simulation due to the reversal of in-phase (s) and out-of-phase (a) modes for 2L3S (Table 2).

Table 3. Summary of Experimental IR and VCD Spectral Data

peptide notation	IR peak frequency and height				VCD peak frequency and sign	
	^{12}C frequency[a,b] (cm^{-1})	^{12}C peak height	^{13}C frequency[a,c] (cm^{-1})	^{13}C peak height	^{12}C part	^{13}C part
unlabeled	0[b]	0.48			1652 (−), 1638 (+), 1623 (−)	
1L	0.5	0.48	0[c]	0.04	1652 (−), 1636 (+), 1620 (−)	
2LT	7.7	0.44	5.7	0.12	1651 (−), 1634 (+)	1603 (−), 1587 (+)
2L1S	−1	0.46	−3.8	0.08	1653 (−), 1638 (+), 1624 (−)	1601 (+), 1587[d] (−)
2L2S	−2	0.45	−3.8	0.07	1654 (−), 1636 (+), 1622 (−)	
2L3S	0.3	0.45	2.9	0.11	1651 (−), 1636 (+)	
2L4S	−1.3	0.42	−2.4	0.04	1656 (−), 1635 (+), 1622 (−)	1604[d] (+)
3LT	6.7	0.37	6.4	0.18	1649 (−), 1627 (+)	1602 (−), 1580 (+)
3L1S	−0.7	0.39	−3.9	0.06	1649 (−), 1637 (+), 1624 (−)	1603 (+), 1584 (−)
4LT	7.7	0.38	5.5	0.19	1653 (−), 1629 (+)	1600 (−), 1580 (+)
4L1S	−1.3	0.43	−5.2	0.14	1654 (−), 1640 (+), 1627 (−)	1603 (+), 1584 (−)

[a] Frequencies are determined by 2nd derivative of the experimental IR spectra. [b] ^{12}C frequencies (in wavenumber) are referenced to unlabeled peptide for easier comparison (the experimental ^{12}C frequency of the unlabeled peptide is 1629.9 cm^{-1}). [c] ^{13}C frequencies (in wavenumber) are referenced to 1L for easier comparison (the experimental ^{13}C frequency of 1L is 1592.6 cm^{-1}). [d] The frequency is uncertain due to the shape of the VCD peak.

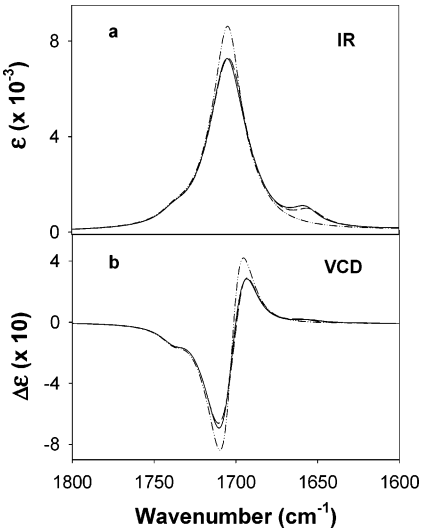

Figure 4. Simulated amide I′ FTIR (a) and VCD (b) spectra for the unlabeled (dash−dotted line −••−••−), 2L2S (dash line − − −) and 2L3S (solid line ——) in the α-helical conformation. The lack of ^{13}C VCD corresponds to the decreased effective coupling.

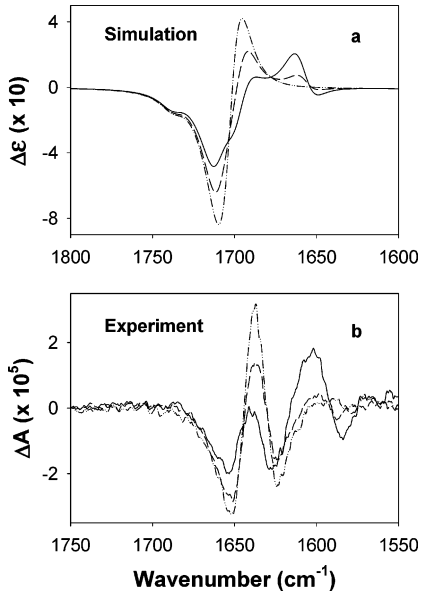

Figure 5. Comparison of simulated helical Ac−A_{24}−$NHCH_3$ (a) and experimental (b) VCD spectra for the unlabeled (dash−dotted line −••−••−), 2L1S (dash line − − −) and 4L1S (solid line ——) peptides at 2 °C. Experimental spectra are normalized to have the same integral amide I peak area.

Although the predicted ^{13}C VCD signal for the alternate (2L1S) isotopic labeling pattern has a predicted intensity comparable to that of the sequential (2LT) pattern, for longer separations such as for 2L2S and 2L3S the predicted ^{13}C VCD intensity diminishes effectively to baseline (only a residual extremely weak positive feature remains, Figure 4). In such a case, the predicted VCD is almost like that of the unlabeled peptide. Experimentally, the VCD for peptides with labels separated by two or three residues (2L2S, 2L3S) is drastically lower in intensity compared to 2L1S having no reliably identifiable VCD in the ^{13}C amide I region (data not shown). This difference in 2L1S and 2L2S does suggest that mechanical coupling may strongly influence VCD.

Increasing the number of labeled residues in a peptide naturally increases the IR and VCD intensity of the ^{13}C band, as we have shown in our previous study of 20 residue helical peptides with four sequential labels.[24] It also disrupts the ^{12}C coupling, causing other effects, which can result in a nonlinear change of the relative ^{12}C−^{13}C intensity.

The IR results for helical peptides with three or four sequentially substituted labels closely reflect the positions of the ^{12}C and ^{13}C bands found with two sequential labels (Table 3, compare 2LT, 3LT, 4LT). The same is true of three or four alternate labels (separated by one ^{12}C) as compared to two alternate labels (see Table 3, compare 2L1S, 3L1S, 4L1S). These experimental patterns are in full agreement with the corresponding simulations (Table 2). For VCD, increasing the number of sequential residues results in ^{12}C and ^{13}C couplets retaining the same sign pattern and in the ^{13}C VCD having somewhat increased intensity for three and four labels. On the other hand, for alternately spaced labels, the VCD of the ^{13}C band grows fast with respect to the ^{12}C band, which in turn becomes more complex. This is a result of alternately spaced ^{12}C residues in the center of the helix whose contributions tend to cancel that of the terminal residues with sequential relationships. Comparison of the simulated and experimental VCD spectra for the unlabeled, 2L1S and 4L1S in Figure 5, shows good agreement for 4L1S on a qualitative basis and confirms the frequency positions assigned to the ^{13}C VCD in Figure 3.

All the calculated spectra are for idealized helical molecules and are compared to experimental data for our 25 residue model system obtained at ∼2 °C. As temperature is increased, the helix

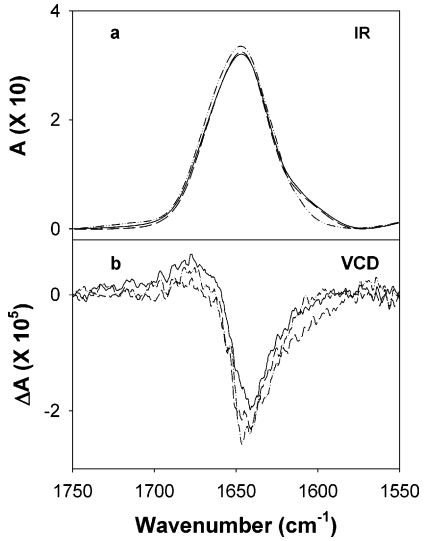

Figure 6. Amide I′ FTIR (a) and VCD (b) spectra for the unlabeled (dash−dotted line −••−••−), 2LT (dash line − − −) and 2L1S (solid line ——) peptides at 75 °C. Spectra are normalized to have the same integral amide I′ peak area. At high temperature, all peptides are in a coil (unfolded) conformation and the ^{13}C amide I′ bands are broadened. Differentiation between labeling patterns is lost.

is less stable and a transition to a disordered (coil) form is obtained. At high temperatures in the coil form, the variation between these samples is reduced (Figure 6). This again agrees with our simulations based on a left-handed 3_1-helix (which is sometimes termed a 3_2-helix[43]) where, if separated, the ^{13}C labels all have about the same frequency, independent of the number.[24] These disordered peptides give a negative VCD ^{13}C amide I band overlapping the negative lobe of the ^{12}C VCD. Sequential labels in the 3_1-helix are predicted to have a narrower frequency dispersion than for the helix geometry due to reduced coupling, but have the same VCD sign pattern as the alternate ones. This prediction reflects our high-temperature experimental results (Figure 6).

Discussion

Two Label Systems. This study of labeled helical peptides directly addresses the coupling of individual residues and the ability of selected isotopic labels to probe conformations of specific sites in a peptide sequence. The concept of coupling between peptide residues has become central to structural interpretation of new Raman and time-dependent IR experiments on small peptides.[11,18−20] In such experiments, both the geometry and interactions are unknown, whereas for the experiments presented here, because the peptides studied are highly helical at low temperatures, the local stereochemistry of the labeled residues is restricted and known. Thus, coupling information derived from study of these peptides provides a control on the structural data being developed with other vibrational techniques.

The key to interpreting the results is their fit to the theoretical modeling. In our simulations, the pattern of modes corresponding to the coupled ^{13}C-labeled residues is clear. Increased separation decreases the coupling, and the sign of the splitting varies with the angle between the residues, reflecting the sign of the coupling constant. However, the angles between residues with different spacings do not change dramatically, so that distance is the more important issue. Distance damping of the variation in the ^{13}C band position for two labels as compared to the single label position was shown in the previous paper[31] and are summarized in Tables 2 and 3 for both our simulation and experiment. The ^{13}C mode for sequential double labeling is predicted to be high compared to a single label and to be somewhat lower for alternate labels due to the reversal of ordering of the symmetric and asymmetric modes. The overall change in the ^{13}C absorbance maximum is predicted to be 10 cm^{-1}, in almost exact agreement with our experimental observations. A similar reversal of symmetric and asymmetric modes is predicted for comparison of the splitting of ^{13}C labels separated by two and by three residues (2L2S and 2L3S), which are predicted to be below and above the single label position, respectively. However, in this case the FF predicted splitting is so small as to make the difference in their observed frequencies only of the order of 2−3 cm^{-1}, while experimentally it is ∼7 cm^{-1} (Table 3). Overall, these changes in coupling constant, V_{ab}, lead to an apparent oscillation in the position of the predicted ^{13}C band, qualitatively reflecting the experimental pattern reported in the previous paper.[31] This sign reversal of the 2L3S coupling term is not computed using the simple transition dipole coupling (TDC) model, as shown by comparing columns 8 and 9 of Table 2. It appears that the TDC model cannot account for the H-bond contribution between these residues. The quality of agreement in the details of these ^{13}C shifts between theory and experiment and the prediction of the relative splittings on change of position in the sequence provides direct evidence for the high quality of the quantum mechanical (QM) FF we have developed for these peptides. By comparison, these results point out a weakness in relying on the classical TDC model to understand coupling in peptides. Reproducing isotopic shifts to this level of accuracy provides confidence that our ab initio QM-based theoretical methods quite accurately develop a measure of the residue coupling.

The similarity in inter-residue distance and the modest change in angle for two labels separated by one (2L1S) or two (2L2S) residues leads to similar coupling magnitudes and therefore similar splittings, 4−5 cm^{-1}, which is borne out experimentally since their ^{13}C maxima have the same shift (Table 3). This relationship would be consistent with a mechanism dominated by dipole coupling. However, the sign change for two labels separated by two and three residues (2L2S and 2L3S) and the large magnitude differences for sequential vs alternate positioning are indicative of an independent mechanism being operative in some cases. As we have shown in a number of previous theoretical[6,8] and experimental[40,44,45] studies, near neighbor, short range interactions provide the dominant coupling mechanism needed for reliable simulation of IR and VCD for a homogeneous peptide. Thus, the sequential case is expected to evidence such mechanical coupling effects. The differences in the effective FF coupling constant and the TDC computed coupling for 2L1S, 2L2S, and 2L3S probably reflect contributions from through bond coupling, though reduced in amplitude.

We have carried out full DFT calculations of the coupling between pairs of *N*-methyl acetamide (NMA) molecules positioned to reflect the relative positions of the (i, i + 2); (i, i +

(43) Van Holde, K. E.; Johnson, W. C.; Ho, P. S. *Principles of Physical Biochemistry*; Prentice Hall: Upper Saddle River, NJ, 1998.

(44) Dukor, R. K. Ph.D. Thesis, Department of Chemistry, University of Illinois at Chicago, Chicago, 1991.

(45) Yoder, G.; Pancoska, P.; Keiderling, T. A. *Biochemistry* **1997**, *36*, 15 123−15 133.

3); (i, $i + 4$) and (i, $i + 5$) pairs of amides in a helix to model the 2L1S, 2L2S, 2L3S, and 2L4S substitutions, respectively. Qualitatively the same pattern results as in Table 2 for the classical TDC calculations. The magnitudes for the NMA modeled coupling approaches the TDC values for 2L3S and 2L4S (and, in contrast to TDC, this model even gets the right sign for 2L3S). However, the 2L1S and 2L2S magnitudes are much larger than for TDC, suggesting that the quantum transitions have an added mechanism for coupling beyond TDC. Certainly for 2LT (i, $i + 1$, which is not possible to model with a DFT calculation for two NMA molecules), there is even more coupling, thus indicating that the contribution of mechanical coupling becomes very important at short range.

The isotopic studies presented here also illuminate the contribution of further separated residues and their relative influence. Although not remeasured in this work, the couplings for separations of up to 7 residues were calculated. In each case, $n = 4-7$, these were of the order of a wavenumber with the symmetric component being lower in frequency. Thus, the predictions both from our FF and from the TDC model dampen the shift to zero with increasing n (except with our FF for 2L3S) and do not fully reproduce the significant cyclic variation as reported experimentally for large separations in the previous paper.[31] This indicates that some smaller interactions, possibly including solvent, are still not represented in our model or that fluctuations in structure might have a more significant impact with larger spacing. The models used here were fully helical to the termini and do not encompass any distortions.

This sign change in coupling constant that results in reversed ordering of the symmetric and asymmetric modes has an even more dramatic effect on the VCD spectrum due to their oppositely signed rotational strengths, $R^{\pm}$. Our simulations predict that the symmetric mode is negative in both the sequential and alternate cases. This leads to the ^{13}C modes having a positive couplet for sequential substitution, just as for the ^{12}C modes, but a negative couplet for alternate substitution, making the VCD pattern opposite that of the ^{12}C. This agrees with the experimental result, which is fully reproducible, though of modest S/N. This sign flip is mathematically self-consistent with our FF results and, in fact, is consistent with the TDC model for 2LT and 2L1S (often termed degenerate coupled oscillator, DCO, for VCD).[41,46] However, the TDC (DCO) results do not predict the correct magnitude for the detectable VCD arising from close lying ^{13}C labels. Considering even further separated labels, for which we have not succeeded in detecting reliable VCD, the TDC (DCO) and FF predicted $R^{\pm}$ values are relatively consistent (the VCD sign variation for 2L2S is for a very small signal). Although reliable ^{13}C VCD is difficult to obtain for 2L3S, we do detect a sharp reduction in the intensity of the low-frequency negative VCD that originates in the ^{12}C residues. This change would be consistent with its overlapping a positive VCD from a negative couplet originating in the ^{13}C mode for 2L3S, which might be expected from the sign flip predicted by our FF model.

From the aspect of helical chirality, one could view the sequential substituents as having a right-handed helical sense due to the 100° rotation about the helix axis of an ideal α-helix. However the alternate ^{13}C labels could be viewed as being effectively left-handed due to their 200° rotation per labeled residue (which is equivalent to −160°). This simple picture would then explain the VCD sign reversal of the ^{13}C peaks in 2LT and 2L1S. However, it would not explain the intensity measured nor the observations for isotopomers with larger ^{13}C separations in the sequence. This simple conceptual model for the helical chirality is consistent with our observations for multiple ^{13}C labels, but such consistency should be expected from the dominance of near neighbor interactions, which are predicted by our FF model.

Multiple Label Systems. Labeled peptides with three and four substituted residues spaced either sequentially or alternately were used to test the generality of these observations and to generate more S/N (especially for VCD) in the ^{13}C bands. In fact, the ^{13}C signals with multiple labels do increase in intensity relative to those with two labeled residues, but the effect is not dramatic. In some sense, this is reflected in our earlier work that positioned four sequential labels in a 20 residue peptide,[24] in order to get better S/N as compared to our earlier work in which we could just detect ^{13}C VCD for two labels in a 17 residue peptide.[6,47] However, with four alternate labels, the ^{12}C part of the VCD is also dramatically reduced in intensity and distorted from the simpler substitution patterns. Here, one must remember that by creating an alternate array of ^{13}C labeled carbonyls one necessarily also creates an alternate array of ^{12}C carbonyls which locally would develop VCD intensity of the same sign pattern since these ^{12}C interspersed residues have the same alternate sequence as the ^{13}C ones. Both of these alternating sequences have effectively left-handed coupling and give rise to VCD opposite in sign to that of the ^{12}C residues on the termini, but in the ^{12}C case this would result in spectral overlap. Thus, the overall ^{12}C VCD intensity would be reduced, while the ^{13}C component would build linearly as expected and as seen experimentally (Figure 5). Overall, this might give an impression of a dramatic increase in VCD intensity for the labeled residues, but this can be an illusion. Thus normalization to an integrated intensity is vital for comparison.

Conclusion

This work has shown that ^{13}C labels on the amide C═O can lead to selective coupling of labeled residues whose spectra are indicative of structure, particularly for VCD. Thus such labeled residues truly form isolated probes of the peptide conformation but do it via their coupling of like-labeled residues. The frequency patterns in the IR are sensitive to the relative positions of the isotopic labels. Separating the ^{13}C specific labels leads to larger separation of the intense component from the ^{12}C peak, which can enhance analytical sensitivity as noted in the previous paper. However, placing the labels together increases their coupling, which enhances their stereochemical sensitivity. Both in VCD and IR the ^{13}C peak intensity is sharply diminished (to become just a shoulder on the ^{12}C peak) when the peptide is thermally disordered. This response is consistent with theoretical predictions for a left-handed 3_1-helix (poly proline II-like). The other aspect that becomes clear from this work is that the TDC model for residue coupling is too simple for peptide analysis.

(46) Narayanan, U.; Keiderling, T. A. *J. Am. Chem. Soc.* **1983**, *105*, 6406−6410.

(47) Keiderling, T. A.; Silva, R. A. G. D.; Decatur, S. M.; Bour, P. In *Spectroscopy of Biological Molecules: New Directions, 8th European Conference on the Spectroscopy of Biological Molecules*; Greve, J., Puppels, G. J., Otto, C., Eds.; Kluwer Academic Publishers: Enschede, 1999; pp 63−64.

Leaving out the through-bond effects, which are encompassed in our ab initio FF, illustrates that TDC has significant magnitude and some sign errors. For structurally sensitive analyses such as VCD this is critical. These results can also cause one to reevaluate geometrical interpretations now becoming broadly available based on only TDC-derived concepts. It is unclear if scaling to empirical parameters will adequately compensate for neglect of through-bond effects, and it is clear that for other structures, such as β-sheets, such a simple parameter assumption is incomplete.

Acknowledgment. This work was partially supported at UIC by grants from the donors of the Petroleum Research Fund administered by the American Chemical Society and the National Science Foundation (CHE03-16014). That at Mt. Holyoke was supported by grants from the National Science Foundation (CHE99848444), and National Institutes of Health (R15GM54334). We thank Dr. Petr Bour for help with theoretical analyses.

JA037998T